Research on Engineering Structures & Materials

www.jresm.org

Research Group

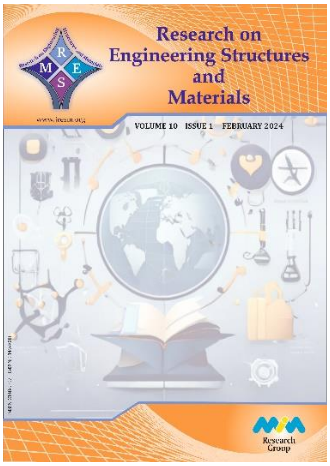

Wind-induced torsional loads and responses of tall buildings

Ashish Singh, Denise-Penelope N. Kontoni, Sasankasekhar Mandal

Online Publication Date: 10 March 2024

URL: http://www.jresm.org/archive/resm2024.08st1011rv.html

DOI: http://dx.doi.org/10.17515/resm2024.08st1011rv

Journal Abbreviation: *Res. Eng. Struct. Mater.*

To cite this article

Singh A, Kontoni DPN, Mandal S. Wind-induced torsional loads and responses of tall buildings. *Res. Eng. Struct. Mater.*, 2024; 10(3): 1281-1300.

Research on Engineering Structures & Materials
www.jresm.org

Review Article

Wind-induced torsional loads and responses of tall buildings

Ashish Singh[1,a], Denise-Penelope N. Kontoni*[2,3,b], Sasankasekhar Mandal[1,c]

[1]*Dept. of Civil Eng., Indian Institute of Technology (BHU), Varanasi, India*
[2]*Dept. of Civil Eng., School of Engineering, University of the Peloponnese, GR-26334 Patras, Greece*
[3]*School of Science and Technology, Hellenic Open University, GR-26335 Patras, Greece*

Article Info

Article history:

Received 11 Oct 2023
Accepted 04 Mar 2024

Keywords:

Tall building;
Wind load;
Wind-induced torsional load;
Wind tunnel experiments

Abstract

High-rise structures are prone to wind-induced forces. Wind load can be resolved into three parts: along-wind load, across-wind load, and torsional wind load. There are well-developed and reliable methods for calculating wind-induced loads in the along-wind direction for tall buildings. Numerous methods are also available to estimate the across-wind load, but this is not the case for the wind-induced torsional load. Researchers have extensively investigated the torsional behavior of tall buildings using wind tunnel experiments and full-scale investigations. This paper attempts to compile the current understanding of the wind-induced torsional response of tall buildings. The present study contributes to realizing the effects of wind-induced torsional loads on tall buildings and gives an in-depth understanding through a comparison of past studies.

1. Introduction

Wind forces that fluctuate can cause significant dynamic motion in high-rise buildings. Tall buildings are bound to oscillate in three ways, *viz*., two translational (along-wind and across-wind directions) and one rotational (torsional mode). The wind-induced loads and their components are represented in Fig. 1. Estimation approaches for along-wind loads are well stabilized and dependable for the purpose of the design of tall structures. Numerous methods are also available to evaluate across-wind loads. However, the estimation procedure is still not standardized for the torsional load caused by wind. The torsional loads are predominantly dynamic in nature. Torsional motions are particularly problematic since, unlike the other components of wind loads, they offer occupants an additional motion due to an apparent rotating horizon. Inhabitants of tall buildings are more likely to get disturbed due to torsional motion than due to translational motion [1]. Tamura *et al.* [2] conducted vibration perception tests to assess the habitability of buildings to vibration and pointed out that individuals can detect vibrations lower than their own "perception threshold" through visual or auditory cues. Kwok *et al.* [3] emphasized the importance of education in habitability. According to Kwok *et al.* [4], prolonged exposure to large-amplitude vibrations can cause dizziness, migraines, and nausea in tall building occupants. Wind-induced torsional vibration can increase displacement and acceleration at the edges of tall buildings. In addition to elevating the wind-induced loads on the primary wind-resistant structure, torsion can also trigger the swaying of outer walls. This, in turn, can impact the integrity of the curtain wall system and lead to increased wind-induced movements [5]. In buildings having longer torsional

*Corresponding author: kontoni@uop.gr
[a]orcid.org/0000-0001-7907-6179; [b]orcid.org/0000-0003-4844-1094; [c]orcid.org/0000-0002-5495-3793
DOI: http://dx.doi.org/10.17515/resm2024.08st1011rv

periods of vibration due to the existence of high eccentricities among the centers of rigidity, the center of mass, and aerodynamic forces, the wind-induced torque tends to be accentuated. The key reason for the development of torsional response is the non-coincidence of the mass center and elastic center of tall buildings.

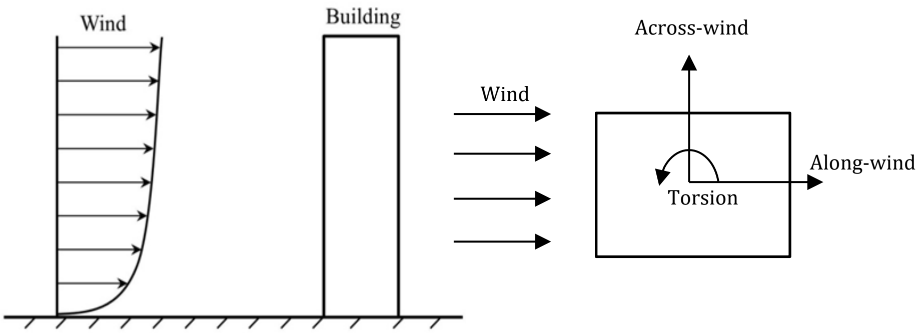

Fig. 1. Direction of wind loading and its components

A tall building can be subjected to wind-induced torsional load in three ways: (i) Due to its structural and architectural characteristics (non-symmetric cross-section, non-symmetrical mass and stiffness distribution), assuming wind load on a building is uniformly distributed across its faces, (ii) Due to the flow characteristics of the wind (uneven pressure distribution across the face, flow approaching at an oblique angle to the face) regardless of plan and shape of the building, and (iii) Due to Dynamic responses resulting into torsion of building. A schematic diagram (Fig. 2) illustrates the causes of wind-induced torsional loads. The most prominent source of wind-generated torsional moments about the vertical axis of the building is the uneven wind pressure distribution on the surrounding surfaces of the building. Torsional motions are particularly problematic since, unlike sway, they subject the occupants to a motion due to an apparent rotating horizon.

The cross-sectional shapes of a building predominantly influence the torsional loading. Cheung *et al.* [6] and Beneke & Kwok [7] concluded that the triangular-shaped model yielded a substantially stronger dynamic torsional response than any other shape. Bandi *et al.* [8] tested five modified triangular shapes in a boundary layer wind tunnel under urban flow conditions. They concluded that the helical models had a greater effect on aerodynamic characteristics. According to Boggs *et al.* [9], among the quadrilateral shapes, the parallelogram experiences unusually high torsion. The increase in torsion is of the order of 33% compared to rectangular shapes. The contribution of higher modes to the response of a wind-excited high-rise building other than the fundamental mode is trivial [10].

The vibration of the primary mode in each direction generally dominates a high-rise building's response to winds. It is crucial to evaluate the response at the top of the structure, particularly the corners, because the corners of a building encounter significant torsional response, *i.e.*, excessive strains and human discomfort. According to Kim and Kanda [11], adjusting the sectional shape by varying its cross-section with height could alter the flow pattern around the models, consequently decreasing wind-induced excitation. Notably, buildings having varying cross-sections with height (tapered and set-back) experienced a more significant torsional moment in urban terrain than in open terrain. Kareem [12] ascertained that the torsional response of symmetric building adds significantly to the overall dynamic response. Also, the combined lateral and torsional kinematics further enhances the building response. Fig. 3 represents the normalized reduced modal spectra of torsional, across-wind, and along-wind forces in an urban environment for a square-section building developed by Kareem [13] in order to estimate the dynamic response of symmetrical and unsymmetrical buildings exposed to wind loads. As shown in Fig. 3, there is a sudden peak in torsional normalized reduced modal spectra at a reduced frequency of 0.10 which emphasizes the importance of torsional wind loading. A high-frequency base balance was used in a wind tunnel by Kijewski and Kareem [14] to compare the different international codes and standards. Moreover, they included cross-wind and torsional responses in their comparison. Liang *et al.* [15] found that torsional vibration contributes significantly to the dynamic response of buildings whose torsional stiffness was close to the lateral stiffness. According to Kim *et al.* [16], tapered and setback buildings (square cross-section), that had offsets in the windward diagonal direction, exhibited an increased torsional response, even if the total RMS accelerations were small.

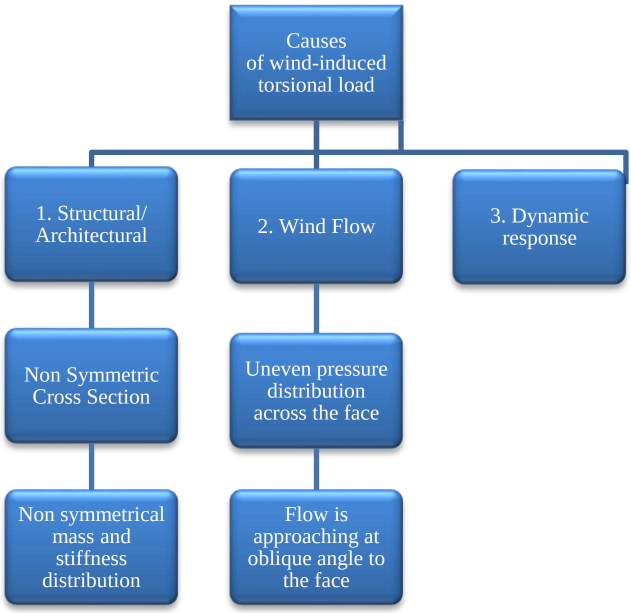

Fig. 2. Causes of wind-induced torsion in tall buildings

Because of the errors associated with modeling, the results of aeroelastic model studies for a structure with a specific geometry and dynamic qualities are difficult to apply to other buildings with identical geometries but distinct dynamic properties [17,18]. Hui *et al.* [19] stated that the mean and fluctuating torsion coefficients were significantly (1.5 times) higher in square buildings (than in rectangular buildings). Several studies of the wind response of tall buildings have been discussed by Hou and Jafari [20]. They also discussed various methodologies to measure the wind-induced response. The design for torsion resistance can be complex and depends on the structural frame's torsional properties. Wind load combinations including torsion were proposed by Stathopoulos *et al.* [21] for rectangular medium-rise buildings. Hu *et al.* [22] studied a high-rise building's translational and torsional responses during Typhoon Khanun. Their findings provide crucial empirical data for improving torsional wind-resistant design in tall buildings.

This paper is an attempt to compile the existing understanding of torsional wind load and responses. Codal provisions concerning torsional wind loading are discussed in section 2. Section 3 deals with wind tunnel tests in which torsional wind load on tall buildings is analyzed. In section 4, various available analytical formulations are reviewed and presented in tabular form. A comparison of the various formulations is also made. Section 5 looks into different available measures for the mitigation of torsional responses. Finally, conclusions from the present study are drawn.

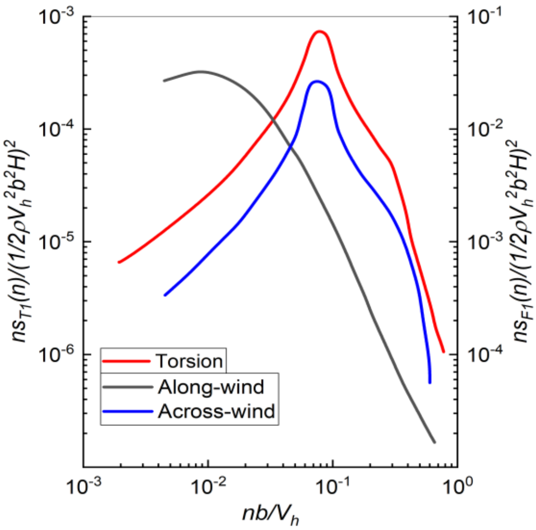

Fig. 3. Normalized reduced modal spectra of torsional, across-wind, and along-wind forces in urban environment for a square building [13]

2. Codal Guidelines on Torsional Wind Loading

Even though various wind tunnel tests have been performed for the estimation of torsional wind loads, very few international codes provide guidelines for incorporating torsional wind loading. A summary of the guidelines for torsional wind loading in some of the existing international wind loading codes is included in this section.

2.1. Japanese Code Guidelines

AIJ 1993 [23] first proposed the torsional wind load provision for tall buildings in the world building codes/standards. The same torsional wind load formula is kept in AIJ 2004 [24]. In addition, ISO 4354 [25] adopted the same formula following [23]. AIJ 2004 [24] dictated the calculation procedure to evaluate the torsional wind load in the design of slender and flexible buildings with $H/\sqrt{BD}$ to be greater than three and $U_H/f_1\sqrt{BD}$ greater than five.

2.2. Indian Code Guidelines

IS 875 (Part 3): 2015 [26] suggests that for tall buildings having unsymmetrical geometry the designs must incorporate torsional effects due to wind pressure. IS 16700:2017 [27] advised that if wind tunnel studies reveal torsional motions, the building's structural system should be modified to minimize these effects, The torsional velocity should be below 0.003 rad/s over the 10-year return period.

2.3. American Code Guidelines

ASCE 7-22 [28] introduces two load scenarios, namely maximum torsion with associated shear and maximum shear with corresponding torsion. According to ASCE 7-22 guidelines, for low-rise buildings, the maximum torsion can be assessed by utilizing 75% of the highest wind loads, along with an equivalent eccentricity of 15% of the building's dimensions.

ASCE 7-22 exempted torsional wind load calculation requirement for buildings with flexible diaphragms. It also stipulated that a building with torsional eccentricity larger than 5% of its width should be avoided in case the buildings have rigid diaphragms. By doing so, the occurrence of large shear forces from torsion effects and the resulting torsional story drift will be prevented, avoiding damage to interior walls and cladding.

2.4. Canadian Code Guidelines

The National Research Council of Canada [29] provides guidelines for the evaluation of the maximum torsion by taking 56% of the maximum wind load with an eccentricity of (15%) of building dimensions.

2.5. European Code Guidelines

The European code [30] considers the maximum torsion as 0.70 of maximum wind load with an additional equivalent eccentricity of 7% of building dimensions.

2.6. Chinese Code Guidelines

GB 50009-2012 [31] introduced provisions for cross-wind and torsional dynamic response into wind load code in 2012. GB 50009-2012 [31] provides the formulation to estimate equivalent wind load induced by torsional dynamic response for rectangular high-rise buildings with $H/\sqrt{BD}$ not more than 6 and the D/B ratio ranging from 1.5 to 5.

2.7. Codal Comparison Study

Elsharawy *et al.* [32] estimated wind-induced torsional load on three tall buildings located in suburban terrain with an aspect ratio of 1 to 3 using the provisions of three international codes. The three codes referred to are the American [33], Canadian [34], and European [30]. A comparison of wind-induced torsional load evaluated from the three codes revealed that there exists wide variability.

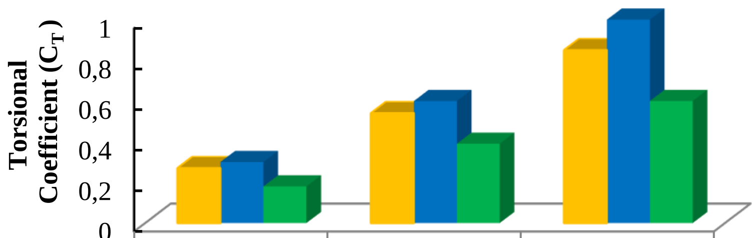

	Side Ratio=1	Side Ratio=2	Side Ratio=3
ASCE 7-10 [33]	0,27	0,54	0,85
NBCC 2010 [34]	0,3	0,6	1
EN 2005 [30]	0,18	0,39	0,6

Fig. 4. Torsional coefficients for buildings (B=30 m, H=60m, L/B=1, 2 and 3)

The evaluated equivalent eccentricity varied from 4.6% [34] to 17.8% [33] and the shear coefficient varied from 1.14 [33] to 1.8. Fig. 4 represents the torsional coefficients for three tall buildings having side ratios 1, 2, and 3. As the side ratio increases, the torsional coefficients also increase. Within the framework of the three standards, the Canadian standard [34] estimates the highest torsional coefficient of all the buildings, while the European standard [30] estimates the lowest torsional coefficient.

3. Wind Tunnel Studies

When assessing the wind load on tall buildings, wind tunnel tests have proven reliable and effective over the past few decades primarily because they can recreate the wind conditions in which tall buildings are immersed.

Initial work in determining the generalized torsional load is attempted by Tallin and Ellingwood [17] based on the wind tunnel data of Reinhold [35]. Applying a linear mode shape, their findings indicated that the RMS value of the real modal torque was 57% of the torque derived from a force balance, and 51% of the torque calculated using a cantilever mode shape. Zou *et al.* [36] carried out a series of wind tunnel tests to study the torsion-induced aeroelastic effect on tall buildings. Nine building models having varying ratios of sides and structural eccentricities are examined. A method has been proposed to calculate the aerodynamic stiffness against torsion and corresponding damping from extensive experimental data. In the absence of structural eccentricity, it is safe to neglect the torsional aerodynamic stiffness ratio. Their study concludes that it is advantageous to align the building face having the longer side normal to the dominant wind. It also observed that the wind-ward eccentricity enhances the torsional dynamic performance, in contrast to leeward eccentricity, which has the opposite effect.

Guzmán-Solís *et al.* [37] tested five rigid scale models in an atmospheric boundary layer wind tunnel to study wind-induced torsional loads on rectangular tall buildings. Each model had the same plan dimensions as the others, but different height aspect ratios. In the wind tunnel, two terrain categories were experimentally generated to evaluate each model under various wind directions. A new parametric equation was proposed based on experimental results to calculate torque coefficients at the base. Their equation includes both the aspect ratio and the wind direction as its variables. Zhang *et al.* [38] studied the stability of wind-excited eccentric tall buildings using an aero-elastic test rig designed for pure torsional vibration. Both the mean and dynamic torsional responses were experimentally studied to assess the predominant effect of the angle of wind incidence. They concluded that at a geometric eccentricity ratio of 10% tall buildings were most susceptible to torsional vibration. It also exhibited a significantly increased maximum mean response. Zhang *et al.* [39] investigated the impact of interference on torsional wind loads. They discovered that in the presence of nearby buildings, the torsional response of a structure can be amplified significantly, reaching up to 2.2 times the response of an isolated tall building model. This phenomenon occurs when the alternating vortex frequency aligns with the fundamental frequency of the building. Using a three-degree-of-freedom aeroelastic tall building model, Tang and Kwok [40] studied the interference mechanisms on both sway and torsional responses. Under an operating reduced wind velocity of 6, for an open terrain wind model, the experimental results concluded that both dynamic torsional and translational responses generally increased under interference effects due to the wakes of upstream buildings. Zou *et al.* [41] estimated wind loads on tall buildings through the study of torsional motion-induced vibrations. They concluded that wind loads in the torsional direction are correlated to the wind loads along and across wind directions. The study emphasized that torsional vibration augments the aerodynamic forces in all three directions, thus resulting in higher wind forces than that measured model. Furthermore, the study revealed that the impact of torsional vibration on aerodynamic forces is more significant at lower reduced wind speeds than at higher reduced wind speeds. Kim *et al.* [42] conducted wind tunnel tests on 13 super-tall building models with atypical building shapes under an urban area flow condition and concluded that the contribution of the torsional moment is almost negligible in super-tall buildings. Tamura *et al.* [43] conducted a study on six different polygon cross-section buildings and concluded that torsional moment coefficients decrease with the increasing number of sides, and the degree of decrease becomes small when the number of sides is larger than

5. Tanaka *et al.* [44] concluded that the torsional moment coefficient decreased for 4-side tapered and set-back building models whose projected area decreased with height.

Most of the wind tunnel studies in the context of torsional loading of tall buildings over the past few decades are summarized in Table 1.

Table 1. Summary of wind tunnel experiments for tall building torsional wind loads

Reference	Geometric Scale	Cross-section	Shape, Full-scale building height	Terrain (α)	Turbulence Intensity at the top of the model (IH)	Measurements	Conclusion
Zhou et al. [45]	1:394	SQ, RC, TR, RM	ST, 200m	0.16, 0.35	-	RMS coefficient of across, along, and torsional wind loads.	Developed an interactive database to calculate the wind-induced response of tall building.
Liang et al. [46]	1:400	SQ, RC	ST, 320m	0.20	7%, 5.5%	Instantaneous fluctuating pressure.	Based on experimental results, proposed empirical formula for torque spectra, RMS torque coefficients, Strouhal number and coherence function of torque.
Thepmongkorn et al. [47]	1:300	RC	ST, 180m	0.15	10%	Perpendicular to the wind, parallel to the wind, and twisting response.	Interference effects from neighboring buildings on the wind response.
Li et al. [48]	1:500	RC	ST, 300m	0.22	12.8%	Instantaneous fluctuating pressure.	Empirical formulae of torque spectra, RMS torque coefficients, and vertical correlation functions.
Yoshie et al. [49]	1:500	RC	ST, 400m	0.14, (1/7)	-	Perpendicular to the wind, parallel to the wind, and twisting response.	Study the vibrational behaviors of different buildings under boundary layer wind.
Hou and Sarkar [50]	1:175	RC	ST, 182.9m	0.34 & tornado	17.7%	Acceleration in X, Y, and torsional direction (Axis is defined on the model).	Measure the wind-induced reactions of tall structures exposed to boundary layer winds versus tornadoes.
Zou et al. [36]	1:400	SQ, RC	ST, 360m	Urban terrain, (Cat C, China)	8%	Wind pressure and displacement response.	Investigate the effect of structural eccentricities on aeroelastic stiffness and damping ratios.
Guzmán-Solís et al. [37]	1:400	RC	ST, 200m	0.15, 0.29	10%, 15%	Shear force, bending moment, and torsion moment at the base of the model.	A new parametric equation is proposed to estimate torque coefficients.
Venanzi et al. [51]	1:500	RC	ST, 182.88 m	-, (open terrain)	-	Across wind base bending moment and Peak base torque.	AIJ provisions overestimate both peak torque and peak across-wind

						bending moments in some cases, resulting in a safe, but economically unfavorable design.
Zou et al. [41]	1:400	SQ, RC ST, 360m	Open terrain (Cat C, China)	10%	Displacements of rims, wind pressure, and angular displacement	Reduced wind speeds and torsional vibration amplitudes represent two significant parameters for aerodynamic forces.

Note: α is the exponent of the power-law, and corresponds to the terrain category; SQ: Square; RC: Rectangular; TR: Triangle: RM: Rhombus; ST: Straight; RD: Rounded Corners; RMS: Root Mean Square.

4. Analytical and Empirical Formulations

Attempts towards an analytical evaluation of the torsional response date back to the 70s, when Patrickson & Friedmann [52] and Fouch & Safak [53] proposed simplified models of the torsional excitation mechanism that did not consider the contributions of the lateral turbulence and the vortex wake. Reinhold and Sparks [54] first conducted wind tunnel as well as full-scale experimental studies on torsional effects on a square section tall building having an H/B ratio of 8.33 and subjected to an urban wind environment. Kareem [10] criticized those procedures that ignore unsteady wake excitation and recommended the use of wind tunnel data for the first time. Isyumov and Poole [55] calculated the mean and dynamic torque components of the circumference of the building using weighted pneumatic averaging. They observed that pressure fluctuations on the back face due to vortex shedding significantly contribute to the dynamic torque and pressure fluctuations on the side face induced by vortex shedding were not significantly contributing to the overall torque. Katagiri *et al.* [56] introduced an analytical approach to assess the lateral-torsional response of tall structures caused by wind forces.

$$T_{max}[U(h)] = \psi\{\bar{T}[U(h)] + g_T T_{rms}[U(h)]\} \tag{1}$$

$$\bar{T}[U(h)] \simeq 0.038\rho L^4 h n_T^2 U_r^2 \tag{2}$$

$$T_{rms}[U(h)] \simeq 0.00167\frac{1}{\sqrt{\zeta_T}}\rho L^4 h n_T^2 U_r^{2.68} \tag{3}$$

$$U_r = \frac{U(h)}{n_T L} \tag{4}$$

$$L = \frac{\int |r|\, ds}{A^{1/2}} \tag{5}$$

Greig [57] proposed an empirical model based on ten aero-elastic model tests, which predicts both the mean and the dynamic torsional response. Equation 1 shows the formula of peak base torque (T_{max}). Expressions of linear base torque ($\bar{T}$) and RMS base torque (T_{rms}) are shown in Equations 2 and 3. In Equations 1 to 5, ψ is a reduction coefficient, ρ is the air density ($\rho \simeq 1.25\ kg/m^3$), h is the height of the building, $g_T \simeq 3.8$ is the torsional peak factor. In Equation 4, U_r is reduced velocity, U(h) is the wind speed at the tip of the building, n_T is the natural frequency and ζ_T is the damping ratio in the fundamental torsional mode of vibration. In Equation 5, L is a shape parameter, ds is the elemental length of the building parameter, and $|r|$ is the torque lever arm of the element ds.

Lythe and Slurry [58] used an experimentally derived database to establish an empirical estimation model for mean torsional loads. Also, they suggested that the large variety of torsion coefficients can be decreased by selecting appropriate normalizing factors and by grouping coefficients as per the reasonable classification of the plan geometry of the building. Liang *et al.* [46] developed empirical formulae for torque spectra, RMS torque coefficients and coherence functions of torque for rectangular tall buildings. These formulae served as the basis for a frequency domain calculation method to estimate wind-induced torsional responses in such buildings. To analyze the torque spectra in rectangular tall buildings with different side ratios, Choi and Kanda [59] introduced a three-term empirical formula. Marukawa & Ohkuma [60] proposed an empirical formula for fluctuating across−wind and torsional forces for prismatic high-rise buildings.

Bazeos & Beskos [61] developed a numerical method to estimate torsional moments due to wind on isolated or a group of rigid buildings of varied cross-sections. While most of the research focused on isolated buildings only, Bazeos & Beskos [61] developed their method for a cluster of buildings as well. Their method uses the boundary elements to take care of the potential flow. Whereas it employs the discrete vortex method to take care of the viscous flow characteristics of the wind. To note, that method works iteratively in the time domain. That method has inherent difficulty in selecting flow separation points in case there is more than one building, especially when the building shapes are complicated.

Based on wind tunnel tests, Li *et al.* [62] proposed empirical formulas for estimating wind-induced torques on L-shaped tall buildings. It takes the side ratio of the building and the terrain category as key variables. Marukawa *et al.* [63] introduced an empirical formula for estimating across-wind and torsional acceleration in high-rise buildings with a rectangular cross-section.

4.1 RMS Torque Coefficients (C_T)

Dynamic wind loads causing torsional motion in tall rectangular buildings can be determined by analyzing torque spectra, RMS torque coefficients, Strouhal number, and the coherence functions of torque. Various researchers have proposed a set of empirical relations for the RMS torque coefficient as shown in Table 2.

Table 2. Various Formulas for RMS Torque Coefficients

Author	RMS Torque Coefficients	RMS Torque Coefficient is dependent on (Variable)	Empirical formula suggested based on experimental investigations
Liang et al. [46]	$\tilde{C}_T = 0.054(D/B)^2 + 0.023$	Side ratio $(\frac{D}{B})$ B= width of windward side, D= depth.	Torque Spectra, RMS torque coefficient, Strouhal Number, and Coherence functions of torque.
Li et al. [48]	$C'_{F_T}(z) = a_1 + (a_2 - a_1)\left(\frac{Z}{H}\right) + (a_3 - a_2)(\frac{Z}{H})^2$	Side ratio $(\frac{D}{B})$	RMS force coefficients, power spectrum densities, and Vertical correlation functions of torsional wind loads.
Guzmán-Solís et al. [37]	$C_T = \dfrac{c_1 + c_2\left(\frac{H}{B}\right) + c_3(\frac{H}{B})^2 + c_4\theta + c_5\theta^2 + c_6\theta^3}{1 + c_7\left(\frac{H}{B}\right) + c_8\theta}$	Wind direction (θ) & height aspect ratio $(\frac{H}{B})$	Parametric equation for estimating torque coefficients at the base of rectangular buildings as a function of wind direction and aspect ratio.

Gui et al. [64]	$C_T'(z) = t_1' + t_2'\left(\frac{z}{H}\right) + t_3'\left(\frac{z}{H}\right)^2$	Side ratio ($\frac{D}{B}$)	The Base root torque coefficient formula is given which is the function of the aspect ratio.
Marukawa & Ohkuma [60]	$C_T = f_{CT1}\left(\frac{D}{B}\right) + f_{CT2}\left(\frac{D}{B}\right).I_{UH}$	Side ratio ($\frac{D}{B}$) and turbulence intensity (IUH).	RMS torque coefficient and overturning moment coefficient.

These empirical relations are dependent on structural parameters like side ratio, and height aspect ratio. Also, they are primarily dependent on wind field parameters such as turbulence intensity and angle of incidence.

4.1.1 Variation of C_T with the Side Ratio

Using the empirical relations given in Table 2 and AIJ 2004 [24], the present study plotted the RMS torque coefficients for various side ratios (D/B) from 0.5 to 2. It is observed from Fig. 5 that Liang *et al.* [46] proposed a formula that gives the maximum values of RMS torque coefficients and Li *et al.* [48] give the lowest values of RMS torque coefficients among the other empirical relations. The results from the proposed empirical relations of Marukawa and Ohkuma [60] & Gui *et al.* [64] are close to AIJ 2004 [24] and these three formulations yield values in between the extremes of Li *et al.* [48] and Liang *et al.* [46].

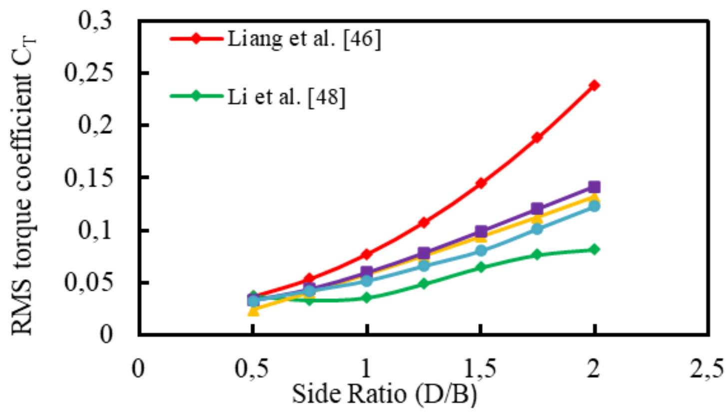

Fig. 5. Comparing the RMS torque coefficients of base torque using different formulations, considering side ratios ranging from 0.5 to 2

4.1.2 Variation of C_T Along the Height

Empirical relations for the variation of RMS torque coefficient along the height proposed by Li *et al.* [48] and Gui *et al.* [64] are compared in Fig. 6. It can be observed from Fig. 6 that C_T is increasing as the D/B ratio increases. C_T is maximum for D/B=2 indicating that oblong buildings having higher depth (dimension of the building along the flow direction) experience maximum torque. For a D/B ratio of one and greater than one, the Gui *et al.* [64] formulation provides higher C_T values than Li *et al.* [48]. However, for a D/B ratio of less than one, the formulation Li *et al.* [48] provides higher C_T values than Gui *et al.* [64]. The Height ratio in the Gui *et al.* [64] study varies from 4.61 to 5.05, whereas, in the study of Li *et al.* [48] height ratio varies from 3 to 4.61.

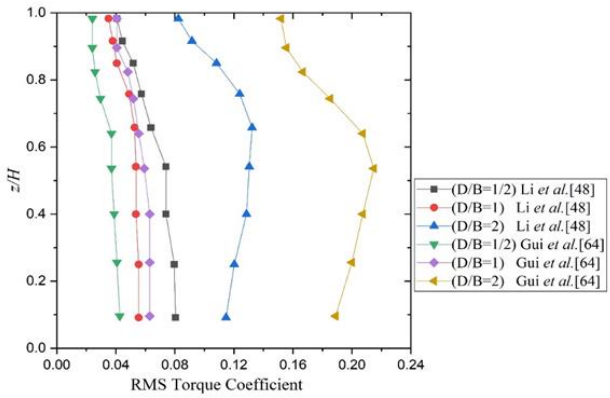

Fig. 6. Comparing the RMS torque coefficients of base torque using different formulations, considering height ratio

4.1.3 Variation of C_T with the Incident Wind Direction

The magnitude and direction of wind force are influenced by topographic features surrounding the building. The Mean and RMS base torsion coefficient are functions of incident wind direction. Guzmán-Solís *et al.* [37] proposed a new parametric equation based on extensive experimental wind tunnel data as shown in Table 2.

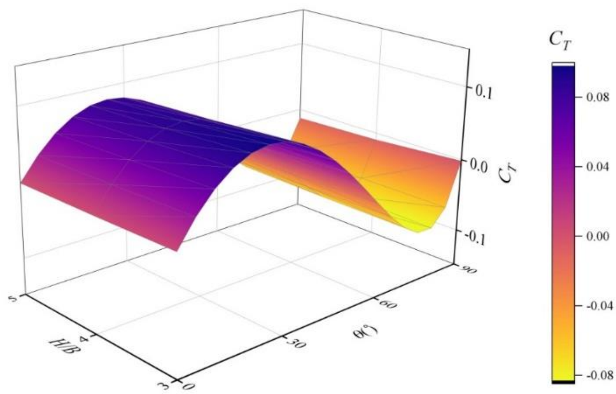

Fig. 7. The 3D plot depicts the variation of the mean torsion coefficient with respect to aspect ratio and wind direction, presenting outcomes derived from the proposed equation by Guzmán-Solís et al. [37]

The variation of C_T has been plotted in Fig. 7 with respect to wind direction as well as height aspect ratio. A similar trend is observed in Fig. 7 for all height aspect ratios. The maximum mean base torque coefficient of 0.1 occurs at 25˚, whereas the minimum of -0.1 occurs at 80°. Bazeos and Beskos [61] reported variation of torsional moment coefficients with varying angles of wind incidence for an isolated square building. Beneke and Kwok [7] investigated the effect of incidence wind angle on mean and dynamic torque for rectangular, diamond, triangular, and D-shaped buildings models. The triangular model at θ=100° yields the largest dynamic response among all the models.

4.2 Power Spectra Density of Torque

The power spectra density of the torque is dependent on both the side ratio and slenderness ratio however Tang *et al.* [65] emphasized that the power spectra density of torque is more sensitive to the side ratio than the slenderness ratio.

Table 3. Various power spectra of the torque

Author	The Power spectra of torque	Range of Side Ratio (D/B) & Aspect Ratio ($\boldsymbol{H/\sqrt{A}}$)
Choi and Kanda [59]	$\frac{f.\,S_m(f)}{\sigma_M^2} = B_2F_1(\psi_1)\left\{\frac{f.\,S_{ST}(f)}{\sigma_{ST}^2} + B_3F_2(\psi_2)\frac{f.\,S_{VS}(f)}{\sigma_{VS}^2} + B_4\frac{fS_{FP}(f)}{\sigma_{FP}^2}\right\}$	$1/3 \le D/B \le 3$, $4.0 \le (H/\sqrt{A}) \le 7.0$
Liang *et al.* [46]	$\frac{nS(n)}{\sigma^2} = A.\frac{1}{d\sqrt{\pi}}exp\left[-\left(\frac{\ln(\bar{n}) - 0.5d^2}{d}\right)^2\right] + (1-A)\frac{C^{0.56}\left(\frac{\bar{n}}{k}\right)^{2.5}}{1.29\left[\left(1-\left(\frac{\bar{n}}{k}\right)^2\right)^2 + C.\left(\frac{\bar{n}}{k}\right)^2\right]}$	$1 \le D/B \le 4$, $4.0 \le (H/\sqrt{A}) \le 8.0$
	$\frac{nS(n)}{\sigma^2} = A_1\frac{C^{0.50}\left(\frac{\bar{n}}{k}\right)^3}{1.56\left[\left(1-\left(\frac{\bar{n}}{k}\right)^2\right)^2 + C.\left(\frac{\bar{n}}{k}\right)^2\right]} + A_2.\frac{1}{d\sqrt{\pi}}exp\left[\left(\frac{\ln(\bar{n}) - 0.5d^2}{d}\right)^2\right] + (1-A_1-A_2).\frac{\bar{n}^2}{8.\left(1+\left(\frac{\bar{n}}{k}\right)^2\right)^2}$	$1/4 \le D/B \le 1$, $4.0 \le (H/\sqrt{A}) \le 8.0$
Li *et al.* [48]	$\frac{fS(f)}{\sigma^2} = \frac{af}{(1+bf^c)^d} + \sum_{j=1}^{N}\frac{K_j(f/F_j)^2}{\left[1-(f/F_j)^2\right]^2 + 4P_j^2(f/F_j)^2}$	$1/2 \le D/B \le 2$, $3.0 \le (H/\sqrt{A}) \le 5$
Gui *et al.* [64]	$\frac{fS_{M_T}(f)}{\sigma_{M_T}^2} = \sum_{i=1}^{2}A_i\frac{S_{pi}\beta_i(f_r/f_{spi})^{\alpha_i}}{\left[1-(f_r/f_{spi})^2\right]^2 + \beta_i(f_r/f_{spi})^2} + A_0\frac{1}{1+\left(ln(f_r/f_{spi})\right)^2}$	$1/3 \le D/B \le 3$, $4.0 \le (H/\sqrt{A}) \le 6.0$

Note: F_1 is an overall shape control function; F_2 has the role of considering negative chordwise correlation characteristics; $S_{FP}(f)$ indicates the second spectral peak; S_{ST} and S_{VS} regular vortex shedding terms; B_1 and B_2 are contribution ratio; A, C, d, and k are coefficients depend on turbulence intensity (I_H) and/or side ratio (D/B) and/or aspect ratio $(H/\sqrt{A})$; $\bar{n} = n/n_s$, $n_s = St.\bar{U}(z)/B$ is the dominant frequency corresponding to the first peak; St is the Strouhal number and $\bar{U}(z)$ is the mean wind speed; a, b, c, d, F_i, P_i, K_i, S_p, β, f_{sp} are parameters that depend on side ratio (D/B); α_1=1, α_2=2

In Table 3, Choi and Kanda [59] provided an empirical formulation to describe the overall characteristics features of torque spectra for a square and rectangular tall building. They suggested that the results from the empirical relations should be compared with experimental data and emphasized the need for parameter sensitivity analysis.

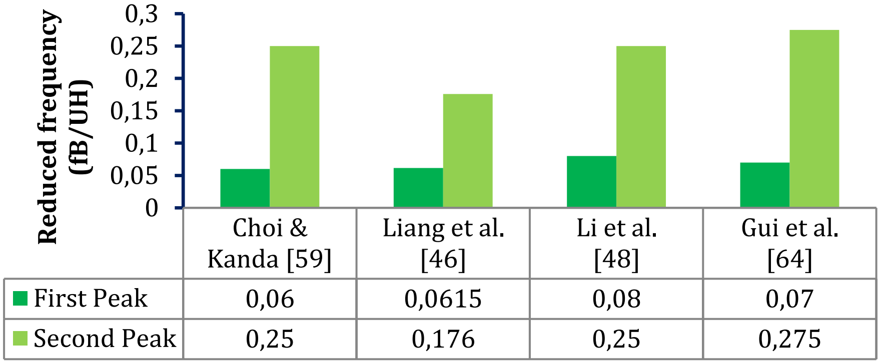

Fig. 8. Reduced frequencies at which first peak and second peaks are obtained

Various formulations have been provided by different researchers on Torque spectra. As it is observed from the plot of various torque spectra it is found that mostly there are two peaks in the curve at two different reduced frequencies. These frequencies are an important parameter for defining the wind environment characteristics. Liang *et al.* [46] stated that among the two peaks, the first is due to asymmetric pressure caused by vortex shedding on the two sides, and the second is due to the reattaching of separated flows. In Fig. 8, reduced frequencies relative to two peaks obtained by various authors are shown. Understanding the first and second peaks of reduced frequencies will be easier with this information.

5. Approaches for Mitigation of Torsional Wind Loads and Responses

A building's response to the wind is mostly determined by its aerodynamic characteristics (design wind speed, turbulence) and its mechanical properties (stiffness, mass, and damping) [66]. Xu *et al.* [67] showed that if the parameters of the tuned mass damper (TMD) were appropriately selected, TMDs were successful in reducing the building's torsional vibration. Kareem *et al.* [68] also mentioned the use of dampers in reducing torsional vibration in their detailed review. Kontoni and Farghaly [69] employed Tuned Mass Dampers (TMDs) to alleviate the impact of wind-induced loads on a steel high-rise structure. Using a smart tuned mass damper, Tse *et al.* [70] evaluated the system's performance and cost efficiency in suppressing wind-induced lateral-torsional movement of tall structures. During full-scale testing, Tamura *et al.* [71] concluded that the tuned liquid damper (TLD) not only showed efficiency but also performed well during strong winds. Ross *et al.* [72] demonstrate that TLD systems can reduce the twisting motions of high-rise buildings significantly. It was concluded by Pozos-Estrada & Hong [73] that peak responses caused by wind-induced torsional load could be reduced by employing TMDs with linear and nonlinear damping mechanisms and also considering correlated wind load effects influences the selection of dampers. Wang *et al.* [74] suggested installing a tuned mass damper-inerter (TMDI)/tuned mass damper (TMD) on a lower floor than the topmost floor to mitigate wind-induced vibration. The new integrated control system (ICS) approach proposed by Akyürek *et al.* [75] is designed with the intent of improving both the safety and performance of buildings with torsional irregularities. The conclusion is drawn that ICS is more robust than TMDs when it comes to limiting inter-story drift. Karami *et al.* [76] proposed a robust method for detecting damage in 3-D shear model structures based on identified Markov parameters and concluded that the controller used could effectively reduce the increase in the torsional response of the structure. In the study conducted by Lei *et al.* [77], the influence of a substantial side-ratio on the wind-induced torsional effects of super high-rise buildings was examined. The investigation yielded significant insights, notably highlighting the efficacy of employing an active tuned mass damper (ATMD) as a viable solution. The ATMD exhibited a dual capability, proficiently mitigating both translational and torsional vibration responses induced by wind forces. That integrated approach holds promising prospects for substantially enhancing structural comfort in the presence of wind-induced vibrations.

Li *et al.* [78] examined the effect of corner chamfers on the aerodynamic performance of tall buildings. Fig. 9 represents the effect of the corner chamfer rate on the RMS torque coefficient. It is evident from Fig. 9, that wind-induced torsional loads decrease as corner chamfer rates increase. However, chamfering is more effective in lessening across-wind load than torsional load. Pozas-Estrada *et al.* [79] compared torsionally sensitive structures with and without linear/nonlinear TMDs subjected to partially correlated wind forces with the probability of not exceeding specified wind-induced motion levels. Their study concluded that a slightly unconservative design is attained in most cases if the correlation between the along-wind force and the torsional moment is ignored in serviceability limit state design checking. Meena et al. [80] conducted a comparison between two regular and two irregular-shaped models. The study concluded that among the four models, the Y-shape model with a rounded corner exhibited the minimum base moment and the lowest coefficient of drag.

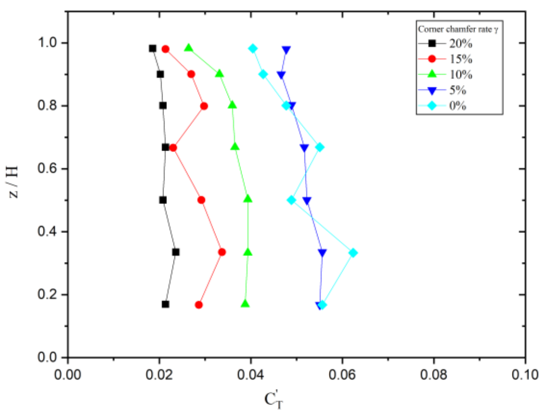

Fig. 9. Comparing the RMS torque coefficients using various chamfer rates ranging from 0-20% [78].

6. Conclusions

This paper summarizes important aspects of torsional wind loads on tall buildings available in the existing literature. There exist numerous studies which deal with the subject matter. It also reviews various methods to evaluate torsional wind load on tall buildings and their development so far.

- Various codal provisions on the torsional wind loads and responses have been emulated as available currently. Provisions of ASCE 07-22, NBCC 2020, and EN-2004 are similar; however, the results calculated differ considerably. The NBCC predicted values of the torsional coefficient are the maximum among the three. Therefore, it is concluded that these codal provisions are not sufficient enough, to evaluate the torsional wind loading. Wind tunnel studies as well as statistical and numerical methods must also be considered.
- Numerous wind tunnel experiments have been conducted to accurately assess torsional wind loads. These studies have mainly considered conventional cross-sections (square, rectangular, *etc.*). Based on the derived data, certain conclusive

theories have been provided, however, further detailed full-scale experimental studies are needed. There is still a need for extensive wind tunnel studies on tall buildings with irregular plans and varying cross-sections along the height.

- Various researchers have derived empirical formulations for the RMS torque coefficient, and torque spectra based on the data obtained from wind tunnel studies. The RMS torque coefficient is expressed in terms of side ratio, height aspect ratio, incident wind direction, and turbulence intensity. All the formulations unanimously found that the RMS torque coefficient increases with the depth dimension of the building. The RMS torque coefficient values attain a maximum at about 0.6 to 0.7 times the height of the building. It is observed from the formulations, that the angle of wind attack is an important parameter to determine the torsion wind loads. The maximum mean base toque coefficient is obtained at an angle of 25 degrees. The paper also lists empirical formulations for the power spectra density of torque.
- Various researchers have suggested the use of Tuned Mass dampers, Tuned liquid dampers, integrated control systems, and different passive measures to reduce the torsional responses. Some authors have also attempted shape optimization approaches to narrow down the torsional wind loads. However, the latter is not as effective as the former one.

This detailed literature study reveals that the simplified methods used to evaluate the torsional wind loads incorporate effective base wind shear and overturning moment. Nonetheless, additional work is needed to deal with wind-induced torsion adequately. The design of buildings may not always consider wind-induced torsional loads, but failing to represent these loads accurately may result in unrealistic spatial variations for design wind loads. In certain circumstances, such exaggerated loads may prove helpful. Proper estimates of wind-induced torsional loads affect the serviceability and long-term functional performance of buildings. Thus, this study concludes that torsional wind load and responses of tall buildings are essential and should not be overlooked during design. Further, the same should be looked into in greater detail through experimental wind tunnel studies and full-scale experiments. It is to be noted that torsional wind loads should be considered for the serviceability of tall buildings.

References

[1] Tallin A, Ellingwood B. Serviceability limit states: wind induced vibrations. Journal of Structural Engineering. 1984;110(10):2424-2437. https://doi.org/10.1061/(ASCE)0733-9445(1984)110:10(2424).

[2] Tamura Y, Kawana S, Nakamura O, Kanda J, Nakata S. Evaluation perception of wind-induced vibration in buildings. Proceedings of the Institution of Civil Engineers-Structures and Buildings. 2006;159(5): 283-293. https://doi.org/10.1680/stbu.2006.159.5.283.

[3] Kwok K C S, Burton M D, Hitchcock P A. Human perception of tall building motions in strong wind environments. The Sixth Asia-Pacific Conference on Wind Engineering (APCWE-IV), Seoul(Korea), pp. 248-262, 2005.

[4] Kwok K C S, Hitchcock P A, Burton M D. Perception of vibration and occupant comfort in wind-excited tall buildings. Journal of Wind Engineering and Industrial Aerodynamics. 2009;97(7-8):368-380. https://doi.org/10.1016/j.jweia.2009.05.006.

[5] Isyumov N, Case P C. Wind-induced torsional loads and responses of buildings. Advanced Technology in Structural Engineering. 2000, pp. 1-8. https://doi.org/10.1061/40492(2000)83.

[6] Cheung J C K, Melbourne W H. Torsional moments of tall buildings. Journal of Wind Engineering and Industrial Aerodynamics. 1992; 42(1-3): 1125-1126. https://doi.org/10.1016/0167-6105(92)90119-U.

[7] Beneke D L, Kwok K C S. Aerodynamic effect of wind induced torsion on tall buildings. Journal of Wind Engineering and Industrial Aerodynamics. 1993;50:271-280. https://doi.org/10.1016/0167-6105(93)90082-Y.
[8] Bandi E K, Tamura Y, Yoshida A, Kim Y C, Yang Q. Experimental investigation on aerodynamic characteristics of various triangular-section high-rise buildings. Journal of Wind Engineering and Industrial Aerodynamics. 2013; 122: 60-68. https://doi.org/10.1016/j.jweia.2013.07.002.
[9] Boggs D W, Hosoya N, Cochran L. Sources of torsional wind loading on tall buildings: Lessons from the wind tunnel. In Advanced Technology in Structural Engineering. 2000: pp. 1-8. https://doi.org/10.1061/9780784404928.
[10] Kareem A, Wind-excited response of buildings in higher modes. Journal of the Structural Division. 1981; 107(4): 701-706. https://doi.org/10.1061/JSDEAG.0005682.
[11] Kim Y, Kanda J. Effects of taper and set-back on wind force and wind-induced response of tall buildings. Wind and Structures. 2010; 13(6): 499-517. https://doi.org/10.12989/was.2010.13.6.499.
[12] Kareem A. Wind induced torsional loads on structures. Engineering Structures. 1981; 3(2): 85-86.
[13] Kareem A. Lateral-torsional motion of tall buildings to wind loads. Journal of Structural Engineering. 1985; 111(11): 2479-2496. https://doi.org/10.1061/(ASCE)0733-9445(1985)111:11(2479).
[14] Kijewski T, Kareem A. Dynamic wind effects: a comparative study of provisions in codes and standards with wind tunnel data. Wind and structures. 1998; 1(1): 77-109. https://doi.org/10.12989/was.1998.1.1.077.
[15] Liang B, Tamura Y, Suganuma S. Simulation of wind-induced lateral-torsional motion of tall buildings. Computers & Structures. 1997; 63(3): 601-606. https://doi.org/10.1016/S0045-7949(96)00356-2.
[16] Kim Y C, Kanda J, Tamura Y. Wind-induced coupled motion of tall buildings with varying square plan with height. Journal of Wind Engineering and Industrial Aerodynamics. 2011; 99(5): 638-650. https://doi.org/10.1016/j.jweia.2011.03.004.
[17] Tallin A, Ellingwood B. Analysis of torsional moments on tall buildings. Journal of wind engineering and industrial aerodynamics. 1985; 18(2): 191-195. https://doi.org/10.1016/0167-6105(85)90097-2.
[18] Shimada K, Tamura Y, Fujii K, Wakahara T. Wind induced torsional motion of tall building. In Proc., 11th National Symposium Wind Engineering. Tokyo (in Japanese), pp. 221-226, 1990.
[19] Hui Y, Tamura Y, Yang Q. Analysis of interference effects on torsional moment between two high-rise buildings based on pressure and flow field measurement. Journal of Wind Engineering and Industrial Aerodynamics. 2017; 164: 54-68. https://doi.org/10.1016/j.jweia.2017.02.008.
[20] Hou F, Jafari M. Investigation approaches to quantify wind-induced load and response of tall buildings: A review. Sustainable Cities and Society. 2020; 62: 102376. https://doi.org/10.1016/j.scs.2020.102376.
[21] Stathopoulos T, Elsharawy M, Galal K. Wind load combinations including torsion for rectangular medium-rise buildings. International Journal of high-rise buildings. 2013; 2(3): 1-11. https://doi.org/10.21022/IJHRB.2013.2.3.245.
[22] Hu J, Li Z, Zhao Z. Field Measurement on Translational and Torsional Wind-Induced Response of a High-Rise Building during Typhoon Khanun. Buildings. 2022;12(10):1698. https://doi.org/10.3390/buildings12101698.
[23] Architecture Institute of Japan (AIJ), Recommendations for loads on buildings, Architectural Institute of Japan. Tokyo. Japan. 1993. (English version: 1996)
[24] Architecture Institute of Japan (AIJ). Recommendations for loads on buildings. Architectural Institute of Japan. Tokyo. Japan. 2004. (In Japanese).

[25] ISO 4354:2009, Second Edition: Wind Actions on Structures; International Organization for Standardization: Geneva. Switzerland. 2009.
[26] IS 875 (Part 3): 2015. Bureau of Indian Standards. Indian Standard Code of Practice for design loads (other than earthquake) for buildings and structures. Part 3 – Wind loads. New Delhi. India 2015.
[27] IS: 16700-2017. Bureau of Indian Standards. Criteria for structural safety of tall concrete buildings. New Delhi. India. 2017.
[28] ASCE/SEI, Minimum design loads for buildings and other structures. ASCE/SEI 7-22, Structural Engineering Institute, Reston, VA, 2022.
[29] NBCC, National Building Code of Canada (NBC). National Research Council of Canada (NRC), Ottawa, Canada, 2020, https://doi.org/10.4224/w324-hv93.
[30] European Committee for Standardization (CEN), Eurocode 1: Actions on structures - Part 1–4: General actions - Wind actions, EN 1991-1-4, Brussels, 2005.
[31] Ministry of Housing and Urban-Rural Development of the People's Republic of China. GB 50009-2012 Load Code for the Design of Building Structures. 2012.
[32] Elsharawy M, Stathopoulos T, Galal K. Evaluation of wind-induced torsional loads on buildings by North American and European codes and standards. In Structures Congress. 2011; pp. 337-348. https://doi.org/10.1061/41171(401)30.
[33] ASCE/SEI. Minimum design loads for buildings and other structures. ASCE/SEI 7-10. Structural Engineering Institute, Reston, VA, 2010.
[34] NBCC, National Building Code of Canada (NBC), User's Guide - NBC 2010 Structural Commentaries (Part 4 of Division B), Canadian Commission on Buildings and Fire Codes (CCBFC), National Research Council of Canada (NRC), Ottawa, 2010.
[35] Reinhold T A. Distribution and correlation of dynamic wind loads. Journal of Engineering Mechanics. 1983; 109(6): 1419-1436. https://doi.org/10.1061/(ASCE)0733-9399(1983)109:6(1419).
[36] Zou L, Li F, Song J, Shi T, Liang S, Mercan O. Investigation of torsional aeroelastic effects on high-rise buildings using forced vibration wind tunnel tests. Journal of Wind Engineering and Industrial Aerodynamics. 2020; 200: 104158. https://doi.org/10.1016/j.jweia.2020.104158.
[37] Guzmán-Solís V, Pozos-Estrada A, Gómez R. Experimental study of wind-induced shear, bending, and torsional loads on rectangular tall buildings. Advances in Structural Engineering. 2020; 23(14): 2982-2995. https://doi.org/10.1177/1369433220927280.
[38] Zhang W J, Xu Y L, Kwok K C S, Torsional vibration and stability of wind-excited tall buildings with eccentricity. Journal of Wind Engineering and Industrial Aerodynamics. 1993; 50: 299-308. https://doi.org/10.1016/0167-6105(93)90085-3.
[39] Zhang W J, Kwok K C S, Xu Y L, Aeroelastic torsional behavior of tall buildings in wakes. Journal of Wind Engineering and Industrial Aerodynamics. 1994; 51(2): 229-248. https://doi.org/10.1016/0167-6105(94)90006-X.
[40] Tang U F, Kwok K C S. Interference excitation mechanisms on a 3DOF aeroelastic CAARC building model. Journal of Wind Engineering and Industrial Aerodynamics. 2004; 92(14-15): 1299-1314. https://doi.org/10.1016/j.jweia.2004.08.004.
[41] Zou L, Xu G, Cai C S, Liang S. Wind tunnel tests of 3D wind loads on tall buildings based on torsional motion-induced vibrations. Wind and Structures. 2016; 23(3): 231-251. https://doi.org/10.12989/was.2016.23.3.231.
[42] Kim Y C, Tamura Y, Tanaka H, Ohtake K, Bandi E K, Yoshida A. Wind-induced responses of super-tall buildings with various atypical building shapes. Journal of Wind Engineering and Industrial Aerodynamics. 2014; 133: 191-199. https://doi.org/10.1016/j.jweia.2014.06.004.
[43] Tamura Y, Xu X, Tanaka H, Ohtake K, Kim Y C, Yoshida A, Yang Q. Effects of configurations of super-tall buildings on aerodynamic and wind-environmental

characteristics. The 2018 World Congress on Advances in Civil, Environmental, & Materials Research (ACEM18, Incheon (Korea), 2018.
[44] Tanaka H, Tamura Y, Ohtake K, Nakai M, Kim Y C. Experimental investigation of aerodynamic forces and wind pressures acting on tall buildings with various unconventional configurations. Journal of Wind Engineering and Industrial Aerodynamics. 2012; 107: 179-191. https://doi.org/10.1016/j.jweia.2012.04.014.
[45] Zhou Y, Kijewski T, Kareem A. Aerodynamic loads on tall buildings: interactive database. Journal of structural engineering. 2003; 129(3): 394-404. https://doi.org/10.1061/(ASCE)0733-9445(2003)129:3(394).
[46] Liang S, Li Q S, Liu S, Zhang L, Gu M. Torsional dynamic wind loads on rectangular tall buildings. Engineering Structures. 2004; 26(1): 129-137. https://doi.org/10.1016/j.engstruct.2003.09.004.
[47] Thepmongkorn S, Wood G S, Kwok, K C S. Interference effects on wind-induced coupled motion of a tall building. Journal of Wind Engineering and Industrial Aerodynamics. 2002; 90(12-15): 1807-1815. https://doi.org/10.1016/S0167-6105(02)00289-1.
[48] Li Y, Zhang J W, Li Q S. Experimental investigation of characteristics of torsional wind loads on rectangular tall buildings. Structural Engineering and Mechanics. 2014; 49(1): 129-145. https://doi.org/10.12989/sem.2014.49.1.129.
[49] Yoshie R, Kawai H, Shimura M, Wei R. A study on wind-induced vibration of super high rise building by multi-degree-of freedom model. Journal of wind engineering and industrial aerodynamics. 1997; 69: 745-755. https://doi.org/10.1016/S0167-6105(97)00202-X.
[50] Hou F, Sarkar P P. Aeroelastic model tests to study tall building vibration in boundary-layer and tornado winds. Engineering Structures. 2020; 207: 110259. https://doi.org/10.1016/j.engstruct.2020.110259.
[51] Venanzi I, Cluni F, Gusella V, Materazzi A L. Torsional and across-wind response of high-rise buildings. In Proceedings of the 12th International Conference on Wind Engineering AWES, Cairns, Australia, 2007.
[52] Patrickson C P, Friedmann P P. Deterministic torsional building response to winds. Journal of the Structural Division. 1979; 105(12): 2621-2637. https://doi.org/10.1061/JSDEAG.0005314.
[53] Foutch D A, Safak E. Tortional Vibration of Along-Wind Excited Structures. Journal of the Engineering Mechanics Division. 1981; 107(2): 323-337. https://doi.org/10.1061/JMCEA3.0002708.
[54] Reinhold T A, Sparks P R. The influence of wind direction on the response of a square-section tall building. Proceedings Fifth International Conference on Wind Engineering. New York, pp. 685-698, 1980.
[55] Isyumov N, Poole M. Wind induced torque on square and rectangular building shapes. Journal of Wind Engineering and Industrial Aerodynamics. 1983; 13(1-3): 183-196. https://doi.org/10.1016/0167-6105(83)90140-X.
[56] Katagiri J, Nakamura O, Ohkuma T, Marukawa H, Tsujimoto T, Kondo K. Wind-induced lateral-torsional motion of a tall building. Journal of Wind Engineering and Industrial Aerodynamics. 1992; 42(1-3): 1127-1137. https://doi.org/10.1016/0167-6105(92)90120-Y.
[57] Greig G L. Towards an estimate of wind-induced dynamic torque on tall buildings. PhD Thesis. University of Western Ontario. London. Canada, 20-40, 1980.
[58] Lythe G R, Surry D. Wind-induced torsional loads on tall buildings, Journal of Wind Engineering and Industrial Aerodynamics. 1990; 36: 225-234. https://doi.org/10.1016/0167-6105(90)90307-X.
[59] Choi H, Kanda J. Proposed formulae for the power spectral densities of fluctuating lift and torque on rectangular 3-D cylinders. Journal of Wind Engineering and Industrial Aerodynamics. 1993; 46: 507-516. https://doi.org/10.1016/0167-6105(93)90318-I.

[60] Marukawa H, Ohkuma T. Formula of fluctuating wind forces for estimation of across-wind and torsional responses of prismatic high-rise buildings. Journal of Structural and Construction Engineering. 1996; 61: 33-42. https://doi.org/10.3130/aijs.61.33_1
[61] Bazeos N, Beskos D E. Torsional moments on buildings subjected to wind loads. Engineering analysis with boundary elements. 1996; 18(4): 305-310. https://doi.org/10.1016/S0955-7997(96)00040-9.
[62] Li Y, Li Q S, Chen F. Wind tunnel study of wind-induced torques on L-shaped tall buildings. Journal of Wind Engineering and Industrial Aerodynamics. 2017; 167: 41-50. https://doi.org/10.1016/j.jweia.2017.04.013.
[63] Marukawa H, Ohkuma T, Momomura Y. Across-wind and torsional acceleration of prismatic high rise buildings. Journal of Wind Engineering and Industrial Aerodynamics. 1992; 42(1-3): 1139-1150. https://doi.org/10.1016/0167-6105(92)90121-P.
[64] Gui Y L I, Qiu-sheng L I, Yi-min D A I. Mathematical models for torsional fluctuating wind loads on rectangular tall buildings. Engineering Mechanics. 2015; 32(6): 177-182. (in Chinese) https://doi.org/10.6052/j.issn.1000-4750.2013.11.1105.
[65] Tang Y, Gu M, Quan Y. Mathematical model of torsional fluctuating wind force on rectangular super-tall buildings. Journal of Building Structures. 2009; 30(5):198-2.4. (In Chinese).
[66] Davenport A G. The response of six building shapes to turbulent wind. Philosophical Transactions of the Royal Society of London. Series A. Mathematical and Physical Sciences. 1971; 269(1199): 385-394. https://doi.org/10.1098/rsta.1971.0039.
[67] Xu Y L, Kwok K C S, Samali B. Torsion response and vibration suppression of wind-excited buildings. Journal of Wind Engineering and Industrial Aerodynamics. 1992; 43(1-3): 1997-2008. https://doi.org/10.1016/0167-6105(92)90623-I.
[68] Kareem A, Kijewski T, Tamura Y. Mitigation of motions of tall buildings with specific examples of recent applications. Wind and structures. 1999; 2(3): 201-251. https://doi.org/10.12989/was.1999.2.3.201.
[69] Kontoni D-P N, Farghaly A A. TMD effectiveness for steel high-rise building subjected to wind or earthquake including soil-structure interaction. Wind and Structures. 2020; 30(4): 423–432. https://doi.org/10.12989/WAS.2020.30.4.423.
[70] Tse K T, Kwok K C S, Tamura Y. Performance and cost evaluation of a smart tuned mass damper for suppressing wind-induced lateral-torsional motion of tall structures. Journal of Structural Engineering. 2012; 138(4): 514-525. https://doi.org/10.1061/(ASCE)ST.1943-541X.0000486.
[71] Tamura Y, Fujii K, Ohtsuki T, Wakahara T, Kohsaka R. Effectiveness of tuned liquid dampers under wind excitation. Engineering Structures. 1995; 17(9): 609-621. https://doi.org/10.1016/0141-0296(95)00031-2.
[72] Ross A S, El Damatty A A, El Ansary A M. Application of tuned liquid dampers in controlling the torsional vibration of high-rise buildings. Wind and Structures. 2015; 21(5): 537-564. https://doi.org/10.12989/was.2015.21.5.537.
[73] Pozos-Estrada A, Hong H P. Sensitivity analysis of the effectiveness of tuned mass dampers to reduce the wind-induced torsional responses. Latin American Journal of Solids and Structures. 2015; 12: 2520-2538. http://dx.doi.org/10.1590/1679-78251856.
[74] Wang Q, Qiao H, De Domenico D, Zhu Z, Xie Z. Wind-induced response control of high-rise buildings using inerter-based vibration absorbers. Applied Sciences. 2019; 9(23): 5045. https://doi.org/10.3390/app9235045.
[75] Akyürek O, Suksawang N, Go T H. Vibration control for torsionally irregular buildings by integrated control system. Engineering Structures. 2019; 201: 109775. https://doi.org/10.1016/j.engstruct.2019.109775.

[76] Karami K, Ahmadi H. Torsional control of asymmetric buildings using online 3-D damage detection and adaptive stiffness devices. Structural Control and Health Monitoring. 2021; 28(10): e2804. https://doi.org/10.1002/stc.2804.
[77] Lei Z H, Bo L I, Wei Z H, Huaibing X U, Ping S H, Xiaohui X U. Research on wind-induced torsional vibration response and vibration control of super-tall building with a large side ratio. Journal of Building Structures. 2023; 4: 87-97. https://doi.org/10.14006/j.jzjgxb.2022.0431.
[78] Li Y, Li C, Li Q S, Song Q, Huang X, Li Y G. Aerodynamic performance of CAARC standard tall building model by various corner chamfers. Journal of Wind Engineering and Industrial Aerodynamics. 2020; 202: 104197. https://doi.org/10.1016/j.jweia.2020.104197.
[79] Pozos-Estrada A, Hong H P, Galsworthy J K. Reliability of structures with tuned mass dampers under wind-induced motion: a serviceability consideration. Wind and Structures. 2011; 14(2): 113-131. https://doi.org/10.12989/was.2011.14.2.113.
[80] Meena RK, Raj R, Anbukumar S. Effect of wind load on irregular shape tall buildings having different corner configuration. Sādhanā. 2022;47(3):126. https://doi.org/10.1007/s12046-022-01895-2.